NASA TECHNICAL NOTE

NASA TN D-3874

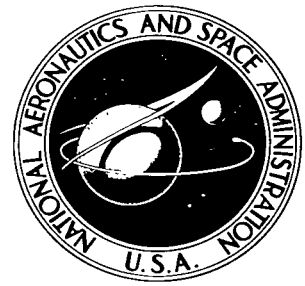

NASA TN D-3874

APPLICATION OF KALMAN FILTERING TO ERROR CORRECTION OF INERTIAL NAVIGATORS

by Heinz Erzberger

Ames Research Center
Moffett Field, Calif.

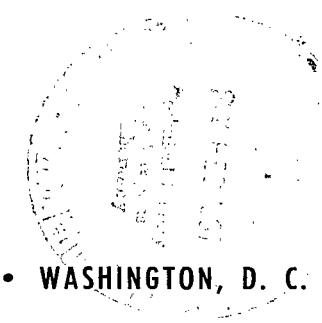

NATIONAL AERONAUTICS AND SPACE ADMINISTRATION • WASHINGTON, D. C. • FEBRUARY 1967

APPLICATION OF KALMAN FILTERING TO ERROR CORRECTION OF INERTIAL NAVIGATORS

By Heinz Erzberger

Ames Research Center
Moffett Field, Calif.

NATIONAL AERONAUTICS AND SPACE ADMINISTRATION

For sale by the Clearinghouse for Federal Scientific and Technical Information
Springfield, Virginia 22151 – Price $2.00

APPLICATION OF KALMAN FILTERING TO ERROR CORRECTION OF INERTIAL NAVIGATORS

By Heinz Erzberger

Ames Research Center

SUMMARY

The design and performance characteristics of an optimum error damping system for an inertial navigator are investigated. The chief component of this system is a Kalman-Bucy filter which gives best estimates of the inertial navigator's errors from noise-contaminated auxiliary velocity or position measurements. The errors estimated by this system include random and constant gyro drift, azimuth, leveling, accelerometer, as well as velocity and position errors. The system also estimates time-correlated errors in the auxiliary navigation measurements which are used to correct the inertial system.

The estimates of error obtained after each measurement from the Kalman-Bucy filter are treated, for the purpose of error reduction of the inertial system, as if they represented exact error values. This procedure of using the estimates as if they represented perfect error measurements is also optimal.

By means of digital computer simulation, the performance of the optimum error damping system was compared, whenever possible, with that of conventional methods. Thus, when an auxiliary velocity is used (e.g., doppler radar), the optimum estimator reduces the inertial position and azimuth error more than 50 percent below the values obtained with the best conventional methods, such as velocity damping or gyrocompassing. The comparative gains made by use of the optimum system depend strongly on the accuracy of both the auxiliary measurement and the initial alinement of the inertial system. But it was generally found that the lower the accuracy of either auxiliary measurement or initial navigator alinement, the better is the performance of the optimum system in comparison to conventional methods.

The performance of an inertial system, optimally updated with auxiliary position measurements, was also studied. The use of auxiliary position measurements, such as LORAN or TACAN, has not previously been exploited in a systematic manner; thus, no performance comparison with conventional methods was possible. It was found that because of the high position accuracy obtainable with these navigation aids, all errors in the inertial system, including azimuth, were strongly reduced. In view of the relatively low cost and general availability of these aids, this result is felt to be especially significant for the projected use of inexpensive inertial systems in commercial jet aircraft.

INTRODUCTION

It is well known that an inertial navigator without periodic updating will eventually make unacceptably large errors. Gyro drift, mechanization, and platform torquing errors invariably degrade the accuracy of the system until, after a period of time, it ceases to be a useful navigation aid. Only at great cost - by careful construction of critical components such as gyros and accelerometers - can its period of usefulness be extended to more than a few hours.

The high cost of accuracy in inertial navigators has led to the use of auxiliary navigation data for controlling the rate of error propagation. Such a system, although no longer purely inertial, often is more economical to construct because of reduced sensitivity to critical components. In addition, it is more versatile than a purely inertial system since it permits at least partial alinement of the navigator in flight.

The most common error-damping scheme in operational aircraft inertial systems is the velocity damped mode, which uses an independent velocity measurement, such as provided by a doppler radar. Other schemes also dependent upon some form of velocity measurement are the gyrocompassing and automatic leveling modes. The analysis of such damped inertial systems is treated elegantly by means of classical feedback control theory in reference 1.

Although the classical theory explains the operation and aids in the design of the system, it is seriously deficient in some aspects. For instance, it does not guarantee that all auxiliary navigation measurements are optimally processed for error damping purposes, nor does it possess an efficient facility for handling measurements contaminated by noise. These and other difficulties with the classical method suggest taking a fresh look at the error damping problem in the context of modern estimation and control theory.

Here the recent work of Bona and Smay on the optimum reset of ship's inertial navigation systems should be mentioned (ref. 2). The present paper differs from theirs in scope and content in that it is slanted more toward aircraft inertial systems.

Essentially, the modern approach separates the error damping problem into two distinct operations of which the first consists of optimally estimating the errors in the inertial system from imperfect measurements, and the second of using the estimated errors to correct the inertial system.

This approach has advantages both in theory and in practice. For instance, random processes in the error model of the inertial system, such as random gyro drift, for example, are handled with ease, as are noise-contaminated navigation measurements. Then, too, there is no limit to the number of sources of auxiliary noisy navigation measurements that can profitably be used for error reduction. Furthermore, the theory provides a simple algorithm for computing the best estimates of all the error states included in the error model. For instance, the algorithm gives a best estimate of

gyro drift rates from position measurements, such as LORAN or TACAN, even though this information may be available only at intermittent time instants. Finally, all sources of auxiliary navigation measurements are processed optimally, in the sense that the mean-square errors in estimating the inertial system errors are minimized.

This paper serves a twofold purpose. First, the design of the optimum estimator and controller is described for a typical inertial system. Then the performance of optimum and classical error damping is compared by means of digital computer simulation. Since the two methods are compared for low and high accuracy inertial systems as well as for different initial alinement conditions, a rather complete picture of the characteristics of the optimum system is obtained.

SYMBOLS

Note: Underlined quantities represent vectors.

$\underline{A}$	specific force vector
C	measurement matrix
F	system matrix
g_m	force per unit mass due to gravity
K_i	Kalman gain matrix
$\underline{k}$	torquer scale factor error (k_x, k_y, k_z)
P_i	covariance of error states at time $i + 1$ given the measurement at time i
P_i'	covariance of error states at time i given the measurement at time i; also, covariance of estimation error
Q_i	covariance of noise for a discrete system
$\tilde{Q}$	covariance of white gaussian system noise
q_ϵ	variance of $u_\epsilon(t)$
R	radius vector from center of the earth to location of navigator
R_i	covariance of measurement noise at time i
$\underline{u}$	system noise vector
$u_\epsilon(t)$	gaussian noise generating random drift rate

$\underline{V}$	true velocity vector
$\underline{V}_d$	difference between inertial and reference velocities
$\underline{V}_r$	reference velocity vector
$\underline{v}$	random velocity reference error (v_x, v_y, v_z)
$\underline{x}$	error state vector
$x_{i\|i}$	optimum error estimate at time i given the measurement at time i
$\underline{z}$	measurement vector
α	inverse of correlation time of accelerometer bias error
β	inverse of correlation time constant of gyro
$\gamma_1, \gamma_2, \gamma_z$	gain constants occurring in classical velocity damped schemes
$\underline{\nabla}$	total accelerometer error (∇_x, ∇_y, ∇_z)
$\underline{\nabla}$	accelerometer bias error
$\underline{\Delta V'}$	inertial navigator velocity error
$\underline{\delta R}$	inertial navigator position error
$\underline{\delta V_r}$	constant velocity reference error
$\underline{\delta V_r'}$	total reference velocity error
$\underline{\delta\theta}$	vector angle relating computer set of axes to true set
$\underline{\epsilon}$	effective gyro drift rate vector (ϵ_x, ϵ_y, ϵ_z)
$\underline{\epsilon}'$	gyro drift rate vector (ϵ_x', ϵ_y', ϵ_z')
$\underline{\epsilon}_c$	effective constant drift rate vector (including gyro torque errors)
ϵ_c'	constant drift rate of a gyro
ϵ_p	polar component of drift rate vector
$\underline{\epsilon}_r$	effective random drift rate vector (including gyro torque errors)
ϵ_r'	random drift rate of a gyro
θ	latitude

$\underline{\rho}$ angular rotation rate of true set of axes with respect to an earth-fixed set

σ^2 steady-state variance of drift rate

$\underline{\Phi}$ vector angle relating platform set of axes to true set

$\Phi(t,\tau)$ transition matrix for error dynamics

$\underline{\Psi}$ vector angle relating platform set of axes to computer set

$\underline{\Omega}$ angular rotation rate of earth with respect to inertial space

$\underline{\omega}$ angular rotation rate of true set of axes with respect to inertial space

$\underline{\omega}_c$ angular rotation rate of computer coordinates with respect to inertial space

$\underline{\omega}_p$ angular rotation rate of platform with respect to inertial space

ω_s Schuler angular frequency

$\bar{(\ )}$ expected value of quantity in parentheses

STATISTICAL MODELS FOR GYRO DRIFT RATE AND ACCELEROMETER ERROR

The error propagation in inertial navigation systems has been studied and documented by many authors (refs. 1 and 3). Several different versions of the error equation exist, but for the purposes of this note the particular form obtained by J. C. Pinson in reference 1 is most suitable. The notation adopted here also conforms as much as possible with that found in reference 1. A brief account of this theory and the notation can be found in appendix A. Although the error equations developed in appendix A suffice when gyro drift rates and accelerometer errors are deterministic time functions, they need to be augmented with additional equations of the error processes when this is not true.

Consider first gyro drift rate $\underline{\epsilon}'$, which is one of the most difficult error sources to control in inertial systems. In the relatively low acceleration environment assumed here the drift rate is generally composed of a constant or bias component and a slowly changing random component. To minimize navigation errors, it is usually necessary, prior to entering the normal navigation mode, to adjust the compensating torques to the gyros so that the total drift rates, constant plus random, are as close to zero as possible. Nonetheless, even with careful adjustment, drift rates of both types will remain. Experience indicates that random drift usually predominates and has the most damaging effect on the navigator accuracy. The random nature of gyro drift has long been recognized, but exhaustive studies of the statistical properties of random gyro drift are difficult to find. However, among the

studies available, the consensus seems to be that random drift rate of a single degree of freedom gyro is exponentially time-correlated (ref. 4). In that case its autocorrelation function has the form

$$G(\tau) = \sigma_r^2 e^{-|\tau|\beta} \tag{1}$$

The correlation time constant $1/\beta$ lies in the neighborhood of 3 to 10 hours for most gyros. This is the basic statistical model for random gyro drift assumed here. Furthermore, if the distribution of the drift rate at any fixed time instant is gaussian, then the Kalman-Bucy theory applies rigorously (ref. 5). A recent statistical analysis of drift data from 50 gyros would tend to support such an assumption (ref. 6). The gaussian assumption is quite convenient, for then it is a simple matter to synthesize a linear dynamical system excited by white gaussian noise so that its output has the desired statistical properties (ref. 5). For the random process considered here the proper choice of system is

$$\frac{d\epsilon_r'}{dt} = -\beta\epsilon_r' + u_\epsilon(t) \tag{2}$$

where ϵ_r' denotes random drift rate. The variance, σ_r^2, of the steady-state drift rate can be shown to be related to the variance, q_ϵ, of the white gaussian noise $u_\epsilon(t)$ by the equation

$$q_\epsilon = 2\beta\sigma_r^2 \tag{3}$$

Since there are three gyros on the stabilized platform, similar dynamical systems are assumed to generate the random drifts for each of the three channels.

The constant drift rate, also known to be present, has not yet been discussed. Although it is not a random process, its value is nevertheless unknown a priori and, therefore, can only be described probabilistically. The distribution of the random variable will again be assumed gaussian with variance σ_c^2. The dynamic system generating this constant random variable is simply

$$\frac{d\epsilon_c'}{dt} = 0 \tag{4}$$

The drift rate model for one gyro is represented in sketch (a).

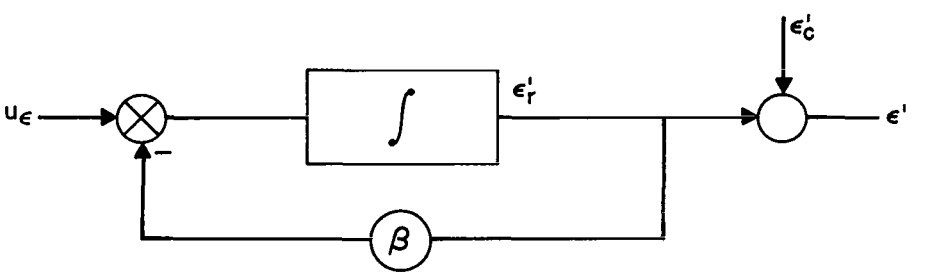

Sketch (a) Dynamic model for gyro drift (one single-axis gyro).

Depending on the characteristics of a particular inertial system, it may be desirable to simplify the proposed drift model. This can easily be done by setting either ϵ_r' or ϵ_c' to zero.

Finally, it is necessary to consider the contribution of torquer scale factor error (k_x, k_y, k_z) to the total drift. As shown in equation (A3), the scale factor error is proportional to the torquing rate $\underline{\omega}$. This error is apparently more difficult to handle than the drift rate $\underline{\epsilon}'$ since $\underline{\omega}$ is a time-varying quantity for a moving navigator. Nevertheless, in real time error estimation no difficulty is encountered. One constructs a statistical and dynamic model for each k, just as for the pure drift rate $\underline{\epsilon}'$ and multiplies k by its respective component of $\underline{\omega}$, which is available in the inertial system's computer. Usually, a simple dynamic model, such as for constant gyro drift, should be sufficient. If $\underline{\omega}$ is not time varying, as in the simulation discussed later, the two sources of drift need not be considered as separate entities, and thus can be represented by a single model, such as shown in figure 1. Henceforth, gyro drift shall mean the total effective gyro drift $\underline{\epsilon}$, appropriately modified to include the scale factor error.

The above discussion on the statistical representation of total gyro drift $\underline{\epsilon}$ applies also to total accelerometer error $\underline{\nabla}$. This error is composed of an offset error and a scale factor error, the latter being proportional to the specific force vector $\underline{A}$ as shown in equation (A10). Generally speaking, accelerometer error is a less serious problem than gyro drift (ref. 1). For example, taken by itself it contributes only a bounded position and velocity error; furthermore, it generally changes less with time than gyro drift. Thus a simple statistical model shown in sketch (b) and similar to the

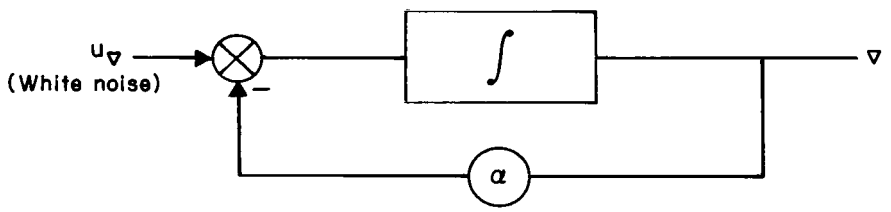

Sketch (b) Dynamic model for error of one accelerometer.

one for random gyro drift is also chosen to represent the total accelerometer error $\underline{\nabla}$. The correlation time $1/\alpha$ depends, of course, on the particular accelerometer, but should lie somewhere between 1 and 20 hours. Strictly speaking, this model generates only the offset error $\underline{\nabla}'$ and not the total error $\underline{\nabla}$ (see eq. (A10)), except when the specific force vector $\underline{A}$ is 0. However, under cruise conditions and a two axes locally level platform mechanization, the average value of $\underline{A}$ along the accelerometer sensitive axes will be small so one is justified in neglecting the scale factor error.

One of the advantages of the Kalman filter over conventional error damping schemes is its ability to account properly for measurement noise. In fact,

if the measurement noise is time correlated, then one can construct a dynamical model of the noise just as was done for gyro drift and estimate the time-correlated part of the noise along with the inertial system errors. A case in point occurs when doppler velocity is used for inertial system error damping. Doppler noise at a fixed reference velocity is composed of a randomly varying component, $\underline{v}$, with correlation time constants in the order of seconds and a constant bias component $\underline{\delta V_r}$. Since both noise components are time correlated, both could be estimated. However, if the sampling interval of the Kalman-Bucy filter is much longer than the correlation time of the noise, it is more efficient to prefilter the doppler signal with conventional smoothing filters. For sampling intervals of a minute or longer, it will still be approximately true that the random noise component of a smoothed doppler signal is uncorrelated. The bias component is easily included in the filter design if the inertial system error model is augmented with the simple dynamic model, developed earlier for a constant random variable, to yield the three equations,

$$\frac{d\delta V_{rx}}{dt} = 0 \ , \qquad \frac{d\delta V_{ry}}{dt} = 0 \ , \qquad \frac{d\delta V_{rz}}{dt} = 0 \tag{5}$$

where $\underline{\delta V_r}$ = column $(\delta V_{rx}, \delta V_{ry}, \delta V_{rz})$ is related to reference velocity $\underline{V_r}$ and true velocity $\underline{V}$ as follows:

$$\underline{V_r} = \underline{V} + \underline{\delta V_r} + \underline{v} \tag{6}$$

In effect, the Kalman-Bucy filter will now estimate the constant reference velocity error along with the inertial system errors.

The next step is to write the entire set of error equations composed of equations (2), (4), (5), (A5), and (A9) as one first-order vector differential equation:

$$\frac{d\underline{x}}{dt} = F\underline{x} + \underline{u} \tag{7}$$

The ordering of the error variables into a state vector $\underline{x}$ is, of course, arbitrary but a logical choice consists of the following arrangement:

$$\underline{x} = \text{column } [\epsilon_{rx}, \epsilon_{ry}, \epsilon_{rz}, \epsilon_{cx}, \epsilon_{cy}, \epsilon_{cz}, \psi_x, \psi_y, \psi_z,$$

$$\nabla_x, \nabla_y, \Delta V_x, \Delta V_y, \delta R_x, \delta R_y, \delta V_{rx}, \delta V_{ry}, \delta V_{rz}] \tag{8}$$

Equation (8) implies the definition $\Delta V_x = \delta\dot{R}_x$, $\Delta V_y = \delta\dot{R}_y$ and the assumption that the vertical channel is not mechanized, that is, $\delta R_z = 0$. The matrix F is, therefore, of dimension 18×18, and its entries are easily determined from the various error equations. Finally, the noise vector $\underline{u}$ has the form

$$\underline{u} = \text{column } [u_{\epsilon x}, u_{\epsilon y}, u_{\epsilon z}, 0,0,0,0,0,0, u_{\nabla x}, u_{\nabla y}, 0,0,0,0,0,0,0] \tag{9}$$

MEASUREMENT EQUATIONS

The purpose of this section is to develop the relationships between the measured error and the error state variables. Such relationships are essential components of the Kalman-Bucy filter theory.

Consider first an external velocity source, such as doppler radar, used as a reference. The doppler radar gives the components of the aircraft velocity vector with respect to the earth in a coordinate frame fixed in the aircraft. The components of this velocity vector are transformed to platform coordinates with the help of the platform resolvers which specify the relative orientation of the two coordinate systems. Since platform and computer frames are nominally identical, inertial and doppler velocity can now be compared.

In general, the resulting difference velocity contains elements of inertial as well as doppler velocity error. The expression for the error of inertial system velocity with respect to an earth-fixed frame can be obtained directly from the equation for $\underline{V}$ derived in reference 1:

$$\underline{V} = \left[\frac{d}{dt}\,\underline{R}\right]_c + \underline{\rho}_c \times \underline{R} \tag{10}$$

where $\underline{\rho}_c$ is the rotation rate of any given set of axes with respect to an earth-fixed set, and the time derivative of $\underline{R}$ is also taken with respect to the given axes. The error in $\underline{V}$, denoted by $\underline{\Delta V}'$, is then obtained from equation (10) by substituting $\underline{R} + \underline{\delta R}$ in place of $\underline{R}$ and identifying terms:

$$\begin{aligned} V + \underline{\Delta V}' &= \left[\frac{d}{dt}\,\underline{\delta R}\right]_c + \underline{\rho}_c \times \underline{\delta R} + \left[\frac{d}{dt}\,\underline{R}\right]_c + \underline{\rho}_c \times \underline{R} \\ &= \underline{\Delta V} + \underline{\rho} \times \underline{\delta R} + \dot{\underline{R}} + \underline{\rho} \times \underline{R} \end{aligned} \tag{11}$$

The right side of equation (11), resolved along some known set of axes, usually the computer set, generates the actual velocity available in the computer. This inertial velocity is to be compared with the reference velocity $\underline{V}_r = \underline{V} - \underline{\delta V}_r'$ where $\underline{\delta V}_r' = \underline{\delta V}_r + \underline{V}$ denotes the total error in the reference velocity. But the existence of an error angle $\underline{\psi}$ between computer and platform axes means that the computer will actually utilize

$$\underline{V} - \underline{\delta V}_r' - \underline{\psi} \times (\underline{V} + \underline{\delta V}_r') \approx \underline{V} - \underline{\delta V}_r' - \underline{\psi} \times \underline{V}$$

in the velocity comparison. Therefore, the difference $\underline{V}_d$ between inertial and reference velocities is

$$\underline{V}_d = \underline{\Delta V} + \underline{\rho} \times \underline{\delta R} + \underline{\psi} \times \underline{V} + \underline{\delta V}_r' \tag{12}$$

In the preceding section the reference velocity error was separated into bias and white noise components and the bias component was included in the inertial

system error model. If this is also done in equation (12), one obtains the final form of the measurement equation

$$\underline{V}_d = \underline{\Delta V} + \underline{\rho} \times \underline{\delta R} + \underline{\psi} \times \underline{V} + \underline{\delta V}_r + \underline{v} \tag{13}$$

where $\underline{v}$ denotes the time-uncorrelated (white noise) component of reference velocity error.[1] Since equation (13) expresses the measured quantity $\underline{V}_d$ as a sum of uncorrelated noise and a linear combination of the error state variables, it can be put in the form required for the Kalman-Bucy theory (ref. 4); that is to say, a 3×18 matrix C can be found which allows equation (13) to be written as

$$\underline{z} = C\underline{x} + \underline{v} \tag{14}$$

Here $\underline{x}$ represents the error state vector and $\underline{z}$ the measured quantity, in this case $\underline{V}_d$.

Another important reference source consists of auxiliary position information such as might be obtained from LORAN, TACAN, or even from visual observation of known landmarks. In the past these measurements, although readily available in many aircraft, have not been fully utilized for error damping of inertial navigators. Yet accurate position information can help considerably in decreasing heading error, as the computer study to be discussed later demonstrates.

The measurement equation for position reference is simply

$$\underline{R}_d = \underline{\delta R} + \underline{v}_p \tag{15}$$

The vector $\underline{v}_p$ represents the reference position error assumed to be white gaussian noise. Obviously, equation (15) can also be written in the form of equation (14).

DESIGN OF THE FILTER

Once the linear dynamic system and the matrix equation relating the state variables of the system with the measured quantities have been determined, the Kalman-Bucy filter can be constructed, provided, of course, that certain statistics, such as the covariances of the system noise and measurement noise and the initial covariance of the state variables, are also known. However, before the filter equations can actually be written, two questions must still be resolved. The first is how the existing filter theory can be made applicable to continuous systems sampled at discrete time instants; and the second is how to use the estimated error states to the best advantage in reducing the inertial system errors.

---

[1]The components of $\underline{v}$ may be correlated with each other, depending on the particular hardware utilized.

The significance of the first question above is best understood by envisioning the sequence of events as they would occur in the system. Suppose a comparison has just been made between inertial velocity and an auxiliary navigation measurement, say doppler velocity. The difference velocity, at whatever time instant it was measured, must be accepted by the filter which must operate upon it and yield a best estimate of the error state. Setting aside for the moment the question what to do with the computed estimate, consider what may happen next at the filter input. Perhaps the aircraft is over water and the doppler signal begins to fade, or in case of position measurement by LORAN, it has just passed outside the range of LORAN stations. In other words, neither the arrival time nor the type of the next measurement is known beforehand. Even if auxiliary navigation measurements were available continuously without interruption, the filter still could accept signals at discrete time instants only, because of the limited computing speed of the digital device which mechanizes the filter equations. The solution to all these difficulties lies, of course, in changing the time-continuous error equations to a discrete system, at least for the purpose of filter design, while at the same time taking care to modify the statistics correctly.

The time discrete system is obtained by expressing the solution of equation (7) in terms of the fundamental matrix $\Phi(t_{i+1},t_i)$ of the system (ref. 7)

$$\underline{x}(t_{i+1}) = \Phi(t_{i+1},t_i)\underline{x}(t_i) + \int_{t_i}^{t_{i+1}} \Phi(t_{i+1},\tau)\underline{u}(\tau)d\tau \tag{16}$$

This equation is written in abbreviated form as follows:

$$\underline{x}_{i+i} = \Phi_i\underline{x}_i + \underline{u}_i \tag{17}$$

To complete the transition from the continuous to the discrete system, it is necessary to calculate the covariance of the random vector $\underline{u}_i$ in terms of the known system parameters and the covariance of $\underline{u}(\tau)$. The covariance Q_i of $\underline{u}_i$ is calculated as follows:

$$Q_i = \int_{t_i}^{t_{i+i}} \int_{t_i}^{t_{i+i}} \Phi(t_{i+1},\tau)\overline{\underline{u}(\tau)\underline{u}^T(t')}\Phi^T(t_{i+1},t')d\tau\, dt' \tag{18}$$

But $\underline{u}(t)$ is a white gaussian random process; hence, its autocorrelation matrix $Q(\tau,t')$ has the form

$$\overline{\underline{u}(\tau)\underline{u}^T(t')} = Q(\tau,t') = \tilde{Q}(\tau,t')\delta(\tau - t') \tag{19}$$

where $\delta(\tau - t')$ is the delta function (ref. 7). Then using equation (19) and a property of the delta function simplifies equation (18) to

$$Q_i = \int_{t_i}^{t_{i+i}} \Phi(t_{i+1},\tau)\tilde{Q}(\tau,\tau)\Phi^T(t_{i+1},\tau)d\tau \tag{20}$$

which gives the desired relation.

With these modifications it is clear that the Kalman-Bucy filter theory for discrete systems is directly applicable here. Since the construction of the filter and the form of the recursion relations for computing the filter parameters are readily available (e.g., refs. 8 and 9), only the final results are included here. Let $\hat{x}_{i|i}$ denote the optimum estimate of $\underline{x}_i$ given the measurement $\underline{z}_i$. The next estimate $\hat{x}_{i+1|i+1}$ is computed from the previous estimate $\hat{x}_{i|i}$ by means of the following relation:

$$\underline{\hat{x}}_{i+1|i+1} = \Phi_i \underline{\hat{x}}_{i|i} + K_{i+1}[\underline{z}_{i+1} - C_{i+1}\Phi_i \underline{\hat{x}}_{i|i}] \tag{21}$$

Here C_{i+1} is the measurement matrix, which is interpreted in equation (21) as the value C assumes at the $(i + 1)$st time instant. The matrix K_{i+1} is called the gain matrix of the filter and is computed recursively as follows:

$$P_i = \Phi_i P'_i \Phi_i^T + Q_i \tag{22}$$

$$P'_{i+1} = [1 - K_{i+1}C_{i+1}]P_i \tag{23}$$

$$K_{i+1} = P_i C_{i+1}^T (C_{i+1} P_i C_{i+1}^T + R_{i+1})^{-1} \tag{24}$$

where

$$P'_i = \overline{(x_i - \hat{x}_{i|i})(x_i - \hat{x}_{i|i})^T} \qquad \text{(covariance of the estimation error at time } i\text{)}$$

$$R_{i+1} = \overline{\underline{v}_{i+1}\underline{v}_{i+1}^T} \qquad \text{(covariance of zero mean measurement noise at time } i + 1\text{)}$$

and P_i is defined by the right side of equation (22). To start the iteration process at $i = 0$, one must have available the a priori statistics P'_0 and $x_{0|0}$.

Now consider the answer to the second question posed at the beginning of this section, namely, how to use the error estimates to the best advantage in reducing the inertial system errors. Since the optimum estimates represent, in a certain sense, the best information available on the error states up to that time, one might argue that the optimum decision after an estimate has been computed consists of resetting every inertial system variable by the amount of the error estimate. Specifically, this procedure would entail subtracting $\delta\hat{R}_x$ from the inertial x coordinate of position immediately after $\delta\hat{R}_x$ has been computed and treating the other variables in a similar manner. That this is indeed the optimum strategy to pursue follows directly from published results on the combined estimation and control problem (ref. 9). In other words, when formulating the error control of an inertial system as a stochastic control problem with the cost function quadratic in the error states, one finds that the solution consists of an independently designed Kalman-Bucy filter for estimating the error states and a controller that operates upon the estimates as if they represented perfect measurements.

Resetting the inertial system variables closes the loop around the Kalman-Bucy filter, all the estimated error states being reduced to zero whenever data are processed by the computer. This procedure simplifies the filter structure because at each step the first and last terms in equation (21) are zero:

$$\underline{\hat{x}}_{i+1|\,i+1} = K_{i+1}\underline{z}_{i+1} \tag{25}$$

Equation (25) holds even if the resetting does not take place instantaneously, so long as it is completed before the next measurement is accepted by the filter.

There is, however, one complication associated with the proposed reset procedure that should be mentioned. It will be remembered that random gyro drift rate ϵ_r and accelerometer bias error ∇ were modeled by dynamic systems of the type shown in sketches (a) and (b). These systems do not actually exist as physical entities; and therefore, it is not possible to reset them physically (i.e., by the conventional method of applying an appropriate control signal at the input of the integrator). The resetting can nonetheless be carried out indirectly by adding a signal to the output variable, which does have physical existence in the inertial navigator. The necessary reset signal is a slowly time-varying quantity dependent upon the dynamical properties of the system. Moreover, it is easy to see that the required signal is generated by a system identical to the one to be reset. For the system shown in sketch (b), for example, the signal which must be added to ∇ is $\hat{\nabla}e^{-\alpha t}$ if an observer at the output is to measure the same response as at the output of a system whose state had been increased instantaneously by an amount $\hat{\nabla}$ at time $t = 0$. This concept is illustrated in sketch (c) below. Obviously the same considerations apply also to the gyro drift model.

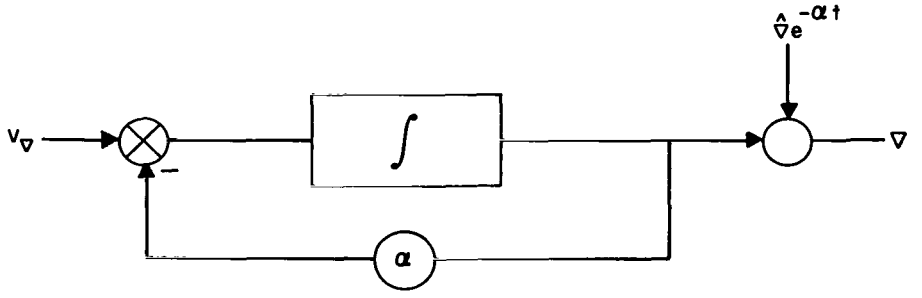

Sketch (c) Accelerometer error model and reset mechanism.

The design of the filter and its relationship with peripheral systems is depicted in figures 1 and 2. Figure 1 shows diagrammatically the sequential computation of the optimum estimate, while figure 2 shows the complete closed loop system, including the simplified calculation of the estimate resulting from the procedure of setting the estimated error state to zero after each estimation. Not shown in the figures are the several logical operations necessary to integrate the filter into the inertial system as a whole. These

operations consist of sensing the type of measurement that has occurred, whether LORAN, TACAN, doppler velocity, or other, programming the computer to calculate the correct gain matrix K_i, and storing the measurement until the gain matrix has been calculated.

Not only are the parameters of equation (17) and of the measurement matrix C time varying, but the latter may even change dimension randomly at the measurement time. The calculation of the gain matrix K_i must, therefore, be done in real time. For the particular kind of problems considered here, it was found that the basic iteration interval should be chosen in the order of a few minutes or less so that the fundamental matrix Φ_i can be approximated by a first degree Taylor series expansion of $e^{F(t_{i+i}-t_i)}$. Also, over such short time intervals it is sufficient to take F constant and update it only at each iteration.

EXPERIMENTAL RESULTS

In this section inertial system error estimation by means of a Kalman-Bucy filter is compared with conventional error damping methods by means of machine computations. The results should help a designer in judging how greatly performance is improved with a Kalman-Bucy filter over conventional methods. Particular care was taken to compare the modern and classical methods under the same conditions so as to assure a fair comparison of the performance characteristics. The machine computations, summarized here in the form of graphs, are essentially time histories of inertial system rms error states calculated for a variety of operating conditions. A conventional locally level, latitude-longitude mechanization was chosen as the model for the inertial system.

Two types of reference sources were considered, doppler velocity and position information. With doppler velocity as a reference, the error state rms values, given by the square root of the diagonal elements of P_i, were calculated for the Kalman-Bucy filter configuration, for velocity damping, automatic leveling and gyro compassing taken together, and for velocity damping alone. Since there are no conventional error damping methods dependent upon position information except for elementary position reset, only the optimum estimator performance was calculated when position information was used. An iteration interval $(t_{i+i} - t_i) = 2.5$ minutes was used for all computations. Also, it was assumed in this study that the vertical channel is not mechanized, so that the position error equation (A9) resolved along the computer set of axes reduces to two scalar equations:

$$\left.\begin{aligned}
\delta\ddot{R}_x + [(\omega_x + \Omega_x)\rho_x + \omega_s^2 + |\underline{\Omega}^2| - |\underline{\omega}^2|]\delta R_x - 2\omega_z\delta\dot{R}_y \\
+ [-\dot{\rho}_z + (\omega_y + \Omega_y)\rho_x]\delta R_y = \psi_z A_y - \psi_y A_z + \nabla_x \\
\delta\ddot{R}_y + [(\omega_y + \Omega_y)\rho_y + \omega_s^2 + |\underline{\Omega}^2| - |\omega^2|]\delta R_y + 2\omega_z\delta\dot{R}_x \\
+ [\dot{\rho}_z + (\omega_x + \Omega_x)\rho_y]\delta R_x = \psi_x A_z - \psi_z A_x + \nabla_y
\end{aligned}\right\} \quad (26)$$

For doppler velocity reference, equation (13) resolved along the computer set of axes yields three scalar equations:

$$\left.\begin{aligned} V_{dx} &= \Delta V_x - \rho_z \delta R_y + \psi_y V_z - \psi_z V_y + \delta V_{rx} + v_x \\ V_{dy} &= \Delta V_y + \rho_z \delta R_x + \psi_z V_x - \psi_x V_z + \delta V_{ry} + v_y \\ V_{dz} &= \rho_x \delta R_y - \rho_y \delta R_x + \psi_x V_y - \psi_y V_x + \delta V_{rz} + v_z \end{aligned}\right\} \qquad (27)$$

Equations (A5) and (26) together with the dynamic models for gyro drift, accelerometer bias, and constant reference velocity error constitute the system equation (7), whereas equation (27) determines the measurement equation (14). Recursion relations (22)-(24) along with the system and measurement equations were employed in calculating the time histories of the rms estimation errors for the optimum estimator. It should be observed that the reset signals do not modify the covariance of the estimation error since they are deterministic (no error in the reset implementation) and, therefore, do not contribute to uncertainties within the system.

The situation is somewhat different for conventional error damping schemes in that both the system equation (7) and the recursion relations (22)-(24) must be appropriately modified. Thus, in the velocity damped mechanization $\gamma_1 V_d$ is added to the left side of the pure inertial mechanization equation (A6), where the gain constant γ_1 is selected to give the desired damping of the transient response (ref. 1). This, in turn, modifies the position error equation (A9) by adding $\gamma_1 V_d$ to its left side. In the automatic leveling mechanization the gyros are precessed at rates $\omega_x - (\gamma_2/R)V_{dy}$, $\omega_y + (\gamma_2/R)V_{dx}$, ω_z, where again γ_2 determines the transient response (ref. 1). In this case $(-\gamma_2/R)V_{dy}$ and $(\gamma_2/R)V_{dx}$ must be added to the right side of the first and second of equations (A5), respectively. Finally the earth-rate gyrocompass mode is obtained by precessing the z gyro at the rate $\omega_z + (\gamma_z/R)V_{dy}$ and the x and y gyros as in the automatic leveling mode. The resulting modification to the ψ equation (A5) is obvious. To compute the covariance of the inertial system error of these configurations, it is only necessary to set the measurement matrix C equal to zero and then use equations (22)-(24) as before.

Two calculated quantities that occur in the figures are platform azimuth error φ_z and polar component of drift rate ϵ_p. Both are linearly related to the chosen error state variables,

$$\varphi_z = \psi_z + \frac{\delta R_x}{R} \tan \theta$$

$$\epsilon_p = \epsilon_y \cos \theta + \epsilon_z \sin \theta \qquad \theta = \text{latitude of navigator}$$

The polar component of drift is important because it produces unbounded ψ components (ref. 1).

In order to check the effect of truncation errors on the calculated values of the K and P' matrices, two FORTRAN programs were written, one in single precision, the other in double precision. Comparison of the matrices calculated by the two programs showed differences at most in the third significant figure after 120 iterations. Single precision should, therefore, suffice to mechanize the iteration equations.

The results of the simulation now to be described are given for three cases: The first corresponds to a poorly alined inertial system equipped with high quality gyros, the second to a well-alined system of the same configuration as used in case 1, and the third case corresponds to a well-alined inertial system equipped with relatively high drift rate gyros. The performance of each case was calculated when operated with competing error damping schemes; namely, optimum filtering and classical velocity damping and gyro compassing. The complete list of parameters specifying each case can be found in tables I-III.

The performance of case 1 is shown in figures 3 and 4 in the form of time histories of rms latitude and azimuth error propagation. Longitude error is not shown, but for this configuration did not differ significantly from latitude error. As is evident from these figures, the performance of the system equipped with an optimum filter surpasses that of the conventionally damped system in both the transient and steady-state phases of the response but the improvement is particularly evident in the transient phase. The strong excitation of the Schuler loop occurring under poor alinement conditions is responsible for the large peaked transients in both figures in the gyrocompass mode (ref. 1). Although this transient in the gyrocompass mode can be reduced by proper choice of the feedback gains γ_1, γ_2, γ_z, it can only be reduced at the detriment of steady-state error in the presence of measurement noise. As the figures demonstrate, this basic shortcoming of the gyrocompass mode is completely overcome with the optimum estimator. Also shown in these figures are the responses of the optimally damped system when updated with position measurements at every iteration step (i.e., at 2.5 min intervals). Azimuth alinement accuracy of this configuration shows the characteristic lag that occurs whenever the estimated quantity is computed from derivatives of measured quantities.

The performance of case 2, the same inertial system as case 1 except that it was assumed more accurately alined initially, is shown in figures 5 and 6. Clearly, the gyrocompass mode was misused in this case, because as seen in figure 6, the azimuth alinement accuracy of the pure inertial system was apparently superior to the steady-state gyrocompass accuracy. While the inflight usefulness of the gyrocompass mode is thus restricted, the optimum estimator does not exhibit this disadvantage since the relative accuracy of the inertial system and the measured data is automatically reflected in the weighting matrix K_i. It is also evident from the figures that the performance improvement gained with an optimum estimator over the velocity damped mode when the inertial system is accurately alined initially is not nearly so striking as in the poorly alined case. Thus, the greatest performance gains can be expected whenever the initial uncertainties of the error states of the inertial system are large. This finding confirms one's belief that statistical analysis increases in value as the disorder in the system increases.

Figures 7-9 show the performance of case 3 which corresponds to an inertial system moving south from north latitude 37.2° with a constant speed of 1700 knots. The rather high gyro-drift rates of this system, given in table III, were chosen in order to evaluate the performance of the estimator when operated with a low-accuracy system. Again, the performance of the estimator surpasses the steady state and transient performance of the conventional velocity damped system by 50 percent or more. Of particular interest is the behavior of the position updated inertial system such as would be provided by LORAN or the proposed navigation satellites. It is interesting to note the high azimuth accuracy attainable with a low accuracy inertial system when high quality position information is available. In comparison to doppler radar, LORAN is a relatively cheap navigation aid, is available over many important air routes and, when used to update the inertial system, can transform an inexpensive, low accuracy inertial system into one of good accuracy.

Figure 9 demonstrates the ability of the estimator to estimate constant gyro drift rate along the polar axis from position or velocity measurements while in flight. The effective constant polar axis drift rate with position updating is reduced by as much as 25 percent from the value of the unaided system. A proportionally larger reduction in drift rate would be obtained with larger initial drift rates. Random drift rate (not shown) is also reduced by about the same percentage. In the past, gyro drift could be measured during flight only with the aid of star trackers.

CONCLUDING REMARKS

The accuracy and versatility of an inertial system can be greatly improved if inertial system errors are optimally estimated with auxiliary noisy navigation measurements. While it is true that the estimator increases the complexity of the inertial system's computer, it is believed that the cost of greater computer complexity can be more than offset because cheaper inertial system components can be used for a specified navigator accuracy. Since an inertial system equipped with an optimum filter estimates all time-correlated errors included in the model, even gyro drift rates and accelerometer bias, from auxiliary navigation measurements, the alinement of the inertial system takes place automatically, on the ground or in the air. The optimally damped system is also far superior to the conventional velocity damped and automatic alinement modes, especially so when the measurements are inaccurate and the initial alinement of the inertial system is poor.

Ames Research Center
National Aeronautics and Space Administration
Moffett Field, Calif., Nov. 29, 1966
125-17-03-02-21

APPENDIX A

INERTIAL SYSTEM ERROR MODEL

This appendix provides a brief review of the inertial system error equations and the notation as used in this paper. A complete derivation can be found in reference 1.

Consider a typical inertial system consisting of a gyro-stabilized platform, three mutually perpendicular accelerometers mounted on the platform, and a computer to solve the mechanization equations of the system. Three coordinate systems enter into the error analysis.

$\hat{l}_{xp}, \hat{l}_{yp}, \hat{l}_{zp}$ unit vectors along the sensitive axes of the accelerometers; also referred to as the platform coordinates

$\hat{l}_x, \hat{l}_y, \hat{l}_z$ unit vectors representing ideal alinement of the inertial system, the true coordinates at the navigator's location

$\hat{l}_{xc}, \hat{l}_{yc}, \hat{l}_{zc}$ computer coordinates

In addition, the following quantities are defined:

$\underline{\omega}$ angular rotation rate of true set of axes with respect to inertial space

$\underline{\omega}_c$ angular rotation rate of computer coordinates with respect to inertial space

$\underline{\omega}_p$ angular rotation rate of platform with respect to inertial space

$\underline{\rho}$ angular rotation rate of the true set of axes with respect to an earth fixed set

$\underline{\delta\theta}$ vector angle relating computer set of axes to true set

$\underline{\varphi}$ vector angle relating platform set of axes to true set

$\underline{\psi}$ vector angle relating platform set of axes to computer set

Clearly the last three quantities are related by the equation

$$\underline{\varphi} = \underline{\psi} + \underline{\delta\theta} \tag{A1}$$

The use of the term vector angle implies that only small angles are of interest; hence, the theory of infinitesimal rotation applies. As is shown in detail in reference 1, the error equations logically fall into two groups, namely, the $\underline{\psi}$ equations and the position error equations. The ψ equation is known to have the following elementary form:

$$\frac{d}{dt}\underline{\psi}\Big]_I = \underline{\epsilon} \tag{A2}$$

where the subscript I indicates that the time derivative of $\underline{\psi}$ is to be taken with respect to an inertial coordinate system. The effective drift rate of the gyros, $\underline{\epsilon}$, is defined as the sum of the actual drift rate, ϵ', and the drift rates contributed by gyro torquer scale factor errors, k_x, k_y, k_z:

$$\underline{\epsilon} = \underline{\epsilon}' + \hat{l}_x k_x \omega_x + \hat{l}_y k_y \omega_y + \hat{l}_z k_z \omega_z \tag{A3}$$

Here ω_x, ω_y, ω_z represent the components of $\underline{\omega}$ in the true coordinate system. The value of $\underline{\omega}$, which is approximated in the computer by $\underline{\omega}_c$, depends upon the particular mechanization as well as the speed and location of the navigator. An especially useful form of equation (A2) is obtained by taking the derivative in a coordinate system rotating with rate $\underline{\omega}$ with respect to inertial space,

$$\frac{d\underline{\psi}}{dt}\Big]_t + \underline{\omega} \times \underline{\psi} = \underline{\epsilon} \tag{A4}$$

and then resolving this equation along the true coordinate axes:

$$\left.\begin{aligned} \dot{\psi}_x + \omega_y\psi_z - \omega_z\psi_y &= \epsilon_x \\ \dot{\psi}_y + \omega_z\psi_x - \omega_x\psi_z &= \epsilon_y \\ \dot{\psi}_z + \omega_x\psi_y - \omega_y\psi_x &= \epsilon_z \end{aligned}\right\} \tag{A5}$$

This is the form of the ψ equation as used here.

The derivation of the position error equations starts first with the writing of the mechanization equation for the particular inertial system that is being studied. This equation is simply Newton's second law written for a rotating coordinate system, and it has the following form (ref. 1):

$$\left[\frac{d^2}{dt^2}\underline{R}\right]_c + 2\underline{\omega}_c \times \left[\frac{d}{dt}\underline{R}\right]_c + \left[\frac{d}{dt}\underline{\omega}_c\right]_c \times \underline{R} + \underline{\omega}_c \times (\underline{\omega}_c \times \underline{R}) - \underline{\Omega} \times (\underline{\Omega} \times \underline{R}) = \underline{A} + \underline{g} \tag{A6}$$

where

R radius vector from the center of the earth to the location of the navigator

$\underline{\Omega}$ angular rotation rate of the earth with respect to inertial space

$\underline{A}$ specific force vector measurable with the accelerometers

$\underline{g}$ $\underline{g}_m - \underline{\Omega} \times (\underline{\Omega} \times \underline{R})$, and $\underline{g}_m$ is the force per unit mass due to gravity

A sufficiently accurate approximation of $\underline{g}$ for the purpose of this paper is given by

$$\left.\begin{aligned} \underline{g} &= -\frac{g}{|\underline{R}|}\underline{R} \qquad g = \text{acceleration of gravity} \\ &= -\omega_s^2 \underline{R} \end{aligned}\right\} \tag{A7}$$

where

$$\omega_s = \sqrt{\frac{g}{|R|}}$$

is the familiar Schuler angular frequency. Errors are introduced in mechanizing equation (A6) first because of the error $\underline{\nabla}$ in the accelerometer outputs, and second because the accelerometers measure acceleration along the platform axes, whereas the computer treats the outputs as though they were measured along the computer axes. The combination of these two effects results in an actual computer input of

$$\underline{A} - \underline{\psi} \times \underline{A} + \underline{\nabla} \tag{A8}$$

instead of the exact value $\underline{A}$. If equations (A7) and (A8) are substituted into equation (A6) along with $\underline{R} + \underline{\delta R}$ in place of $\underline{R}$, one obtains the position error equation by identifying terms:

$$\ddot{\underline{\delta R}} + 2\underline{\omega} \times \dot{\underline{\delta R}} + \dot{\underline{\rho}} \times \underline{\delta R} + [(\underline{\omega} + \underline{\Omega}) \cdot \underline{\delta R}]\underline{\rho} + (\omega_s^2 + |\underline{\Omega}|^2 - |\underline{\omega}|^2)\underline{\delta R} = -\underline{\psi} \times \underline{A} + \underline{\nabla} \tag{A9}$$

Equation (A9) holds for an observer not rotating with respect to the true coordinate system; for any other rotating coordinate system it is only necessary to replace $\underline{\omega}$ with the angular rotation rate, with respect to inertial space, of the new coordinate system.

In a manner similar to gyro drift, one separates the accelerometer error into two components, an offset error, $\underline{\nabla}'$, resulting from incomplete nulling under zero acceleration, and a component resulting from accelerometer scale factor errors k_x', k_y', k_z'.

$$\underline{\nabla} = \underline{\nabla}' + \hat{l}_x k_x' A_x + \hat{l}_y k_y' A_y + \hat{l}_z k_z' A_z \tag{A10}$$

Equations (A4) and (A9) specify the dynamics of error propagation in an inertial system, and they have the advantage over other formulations in that the angle and position error equations are uncoupled. A possibly important error source, which has not been included, is the uncertainty in the calculated Schuler angular frequency ω_s. This error, introduced mainly by altitude error, is the origin of the vertical channel instability (ref. 1). However, here it is assumed that the vertical channel is not mechanized and that altitude is measured with negligible error by auxiliary equipment. Another point to be mentioned is that the analysis presented here gives rise

to the linear error equations whereas a more detailed treatment would show the existence of second degree terms in the error state variables. However, for the relatively small errors and short time intervals of interest here the second degree terms do not contribute significantly to the error propagation.

REFERENCES

1. Pinson, John C.: Inertial Guidance for Cruise Vehicles. Ch. 4 of Guidance and Control of Aerospace Vehicles, C. T. Leondes, ed., McGraw-Hill Book Co., Inc., 1963, pp. 113-187.

2. Bona, B. E.; and Smay, R. J.: Optimum Reset of Ship's Inertial Navigation System. IEEE Trans. Aerospace and Electronic Systems, vol. 2, no. 4, July 1966, pp. 409-414.

3. Broxmeyer, Charles: Inertial Navigation Systems. McGraw-Hill Book Co., Inc., 1964.

4. Dushman, Allan: On Gyro Drift Models and Their Evaluation. IRE Trans. Aerospace and Navigational Electronics, vol. ANE-9, no. 4, Dec. 1962, pp. 230-234.

5. Kalman, R. E.; and Bucy, R. S.: New Results in Linear Filtering and Prediction Theory. Trans. ASME, Series D, J. Basic Engr., vol. 83, no. 1, March 1961, pp. 95-108.

6. Cooper, John R.: A Statistical Analysis of Gyro Drift Test Data. Master Thesis, MIT, Sept. 1965.

7. Zadeh, L. A.; and Desoer, Charles A.: Linear System Theory. McGraw-Hill Book Co., Inc., 1963.

8. Kalman, R. E.: A New Approach to Linear Filtering and Prediction Problems. Trans. ASME, Series D, J. Basic Engr., vol. 82, pt. 2, 1960, pp. 35-45.

9. Joseph, P. D.; and Tou, J. T.: On Linear Control Theory. Trans. AIEE, pt. II, 80, 1961, p. 18.

TABLE I.- ERROR SCHEDULE AND SYSTEM PARAMETERS CORRESPONDING TO CASE 1

Navigator location: 37.2° north latitude; gyro drift rate time constant $1/\beta = 5$ hours; accelerometer bias time constant $1/\alpha = 20$ hours; observation time interval = 2.5 minutes for optimum estimators and continuous for conventional modes; navigator stationary or moving slowly.

The covariance matrix of the error states P' at $t = 0$ was assumed to be diagonal and its rms diagonal elements are listed below; covariance matrix of system noise $\tilde{Q}$ is diagonal and its nonzero elements are computed from the steady-state drift rates and accelerometer bias as $2\sigma_d^2\beta$ and $2\sigma_b^2\alpha$, respectively.

Error state and units	Element of P'	Initial rms
x gyro random drift rate ϵ_{xr}, min of arc/hr	$P'(1,1)$	1.55
y gyro random drift rate ϵ_{yr}, min of arc/hr	$P'(2,2)$	1.55
z gyro random drift rate ϵ_{zr}, min of arc/hr	$P'(3,3)$	1.55
x gyro constant drift rate ϵ_{xc}, min of arc/hr	$P'(4,4)$	1.55
y gyro constant drift rate ϵ_{yc}, min of arc/hr	$P'(5,5)$	1.55
z gyro constant drift rate ϵ_{zc}, min of arc/hr	$P'(6,6)$	1.55
ψ_x, min of arc	$P'(7,7)$	30
ψ_y, min of arc	$P'(8,8)$	30
ψ_z, min of arc	$P'(9,9)$	60
x accelerometer random bias ∇_x, knots/hr	$P'(10,10)$	20
y accelerometer random bias ∇_y, knots/hr	$P'(11,11)$	20
x velocity (latitude) error ΔV_x, knots	$P'(12,12)$	1
y velocity (longitude) error ΔV_y, knots	$P'(13,13)$	1
x position (longitude) error δR_x, nautical miles	$P'(14,14)$	1
y position (latitude) error δR_y, nautical miles	$P'(15,15)$	1
constant x reference velocity error, knots	$P'(16,16)$	2
constant y reference velocity error, knots	$P'(17,17)$	2
constant z reference velocity error, knots	$P'(18,18)$	2

Velocity measurement noise covariance matrix

$$R_i = \begin{bmatrix} 0.25 & 0 & 0 \\ 0 & 0.25 & 0 \\ 0 & 0 & 0.25 \end{bmatrix}, \quad \text{knots}^2$$

Position measurement noise covariance matrix

$$R_i = \begin{bmatrix} 0.25 & 0 \\ 0 & 0.25 \end{bmatrix}, \quad \text{nautical miles}^2$$

Steady state random gyro drift rate (each channel): $\sigma_d = 2$ min/hr
Steady state random accelerometer bias (each channel): $\sigma_b = 20$ knots/hr

TABLE II.- ERROR SCHEDULE AND SYSTEM PARAMETERS CORRESPONDING TO CASE 2

Only changes from table I are listed.

Error state	ϵ_{xr}	ϵ_{yr}	ϵ_{zr}	ϵ_{xc}	ϵ_{yc}	ϵ_{zc}	ψ_x	ψ_y	ψ_z
Initial rms	0.707	0.707	0.707	0.707	0.707	0.707	0.5	0.5	1

TABLE III.- ERROR SCHEDULE AND SYSTEM PARAMETERS CORRESPONDING TO CASE 3

Navigator moves southward from 37.2° north latitude at 1700 knots. Only changes from table I are listed.

Error state	ϵ_{xr}	ϵ_{yr}	ϵ_{zr}	ϵ_{xc}	ϵ_{yc}	ϵ_{zc}	ψ_x	ψ_y	ψ_z
Initial rms	4	4	4	4	4	4	0.5	0.5	1.0

Error state	ΔV_x	ΔV_y	δR_x	δR_y	δV_{rx}	δV_{ry}	δV_{rz}
Initial rms	0.5	0.5	0.5	0.5	6.8	6.8	6.8

Velocity measurement noise covariance matrix

$$R_i = \begin{bmatrix} 26 & 0 & 0 \\ 0 & 26 & 0 \\ 0 & 0 & 26 \end{bmatrix}, \quad \text{knots}^2$$

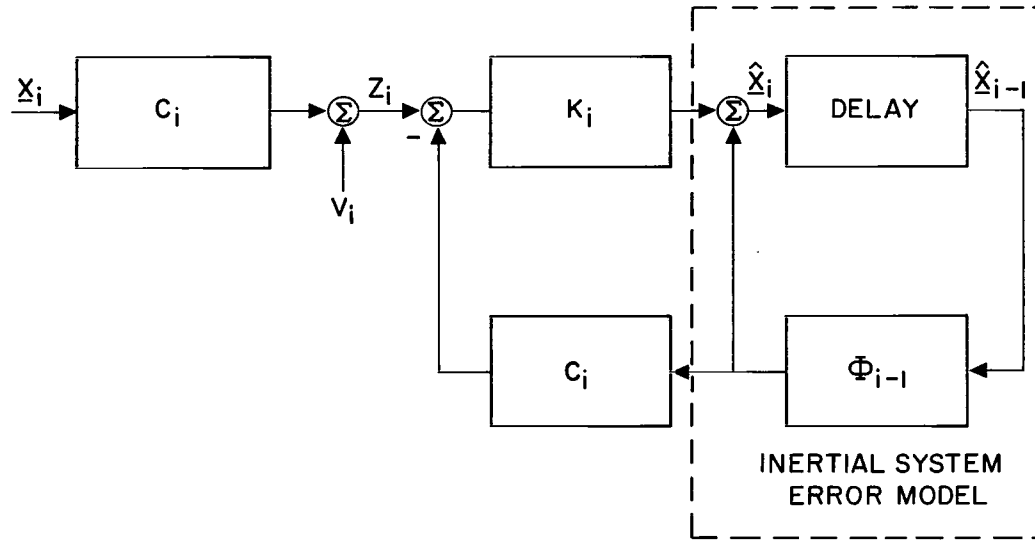

Figure 1.- Schematic representation of the Kalman-Bucy filter.

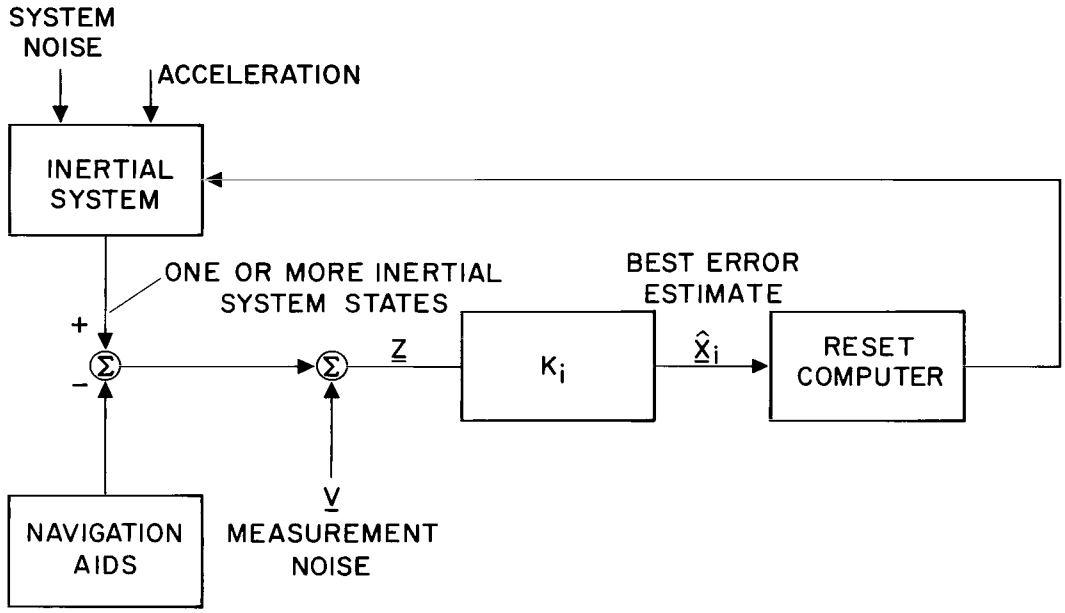

Figure 2.- Block diagram of optimum system.

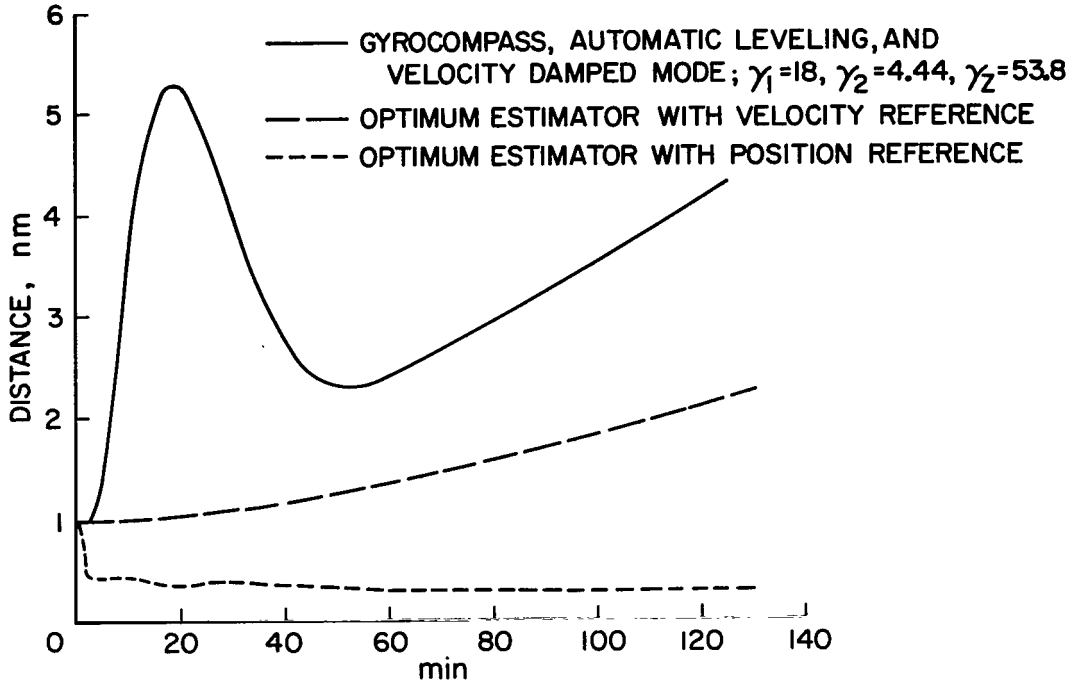

Figure 3.- Propagation of rms latitude (Y axis) error in a poorly alined inertial navigator (case 1).

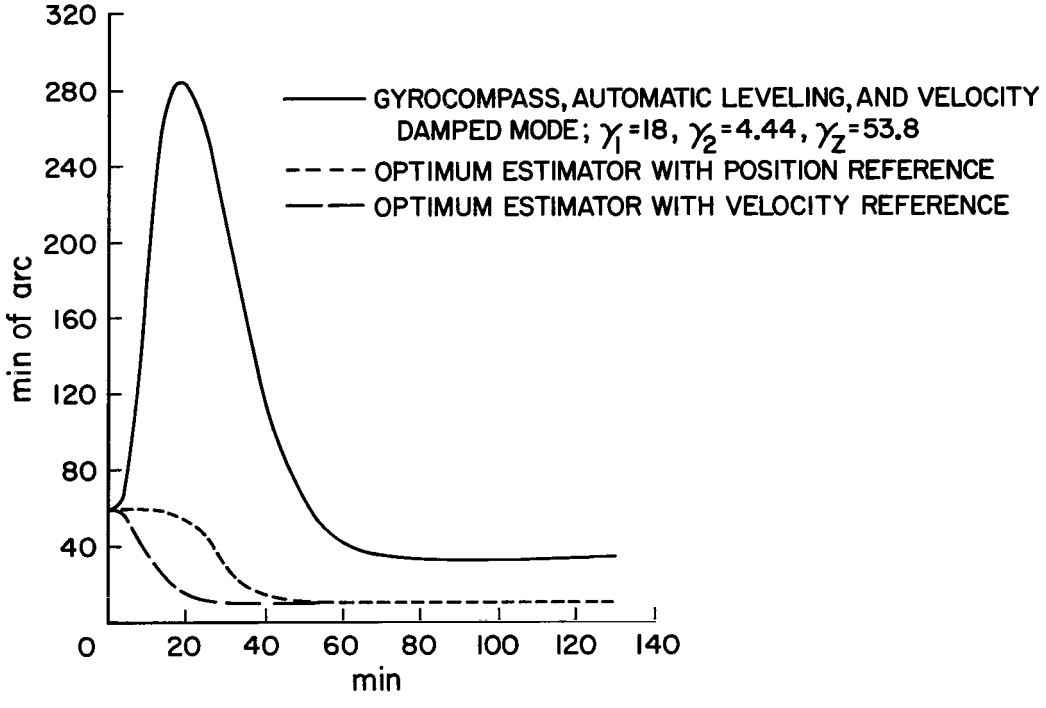

Figure 4.- Propagation of rms azimuth error in a poorly alined inertial navigator (case 1).

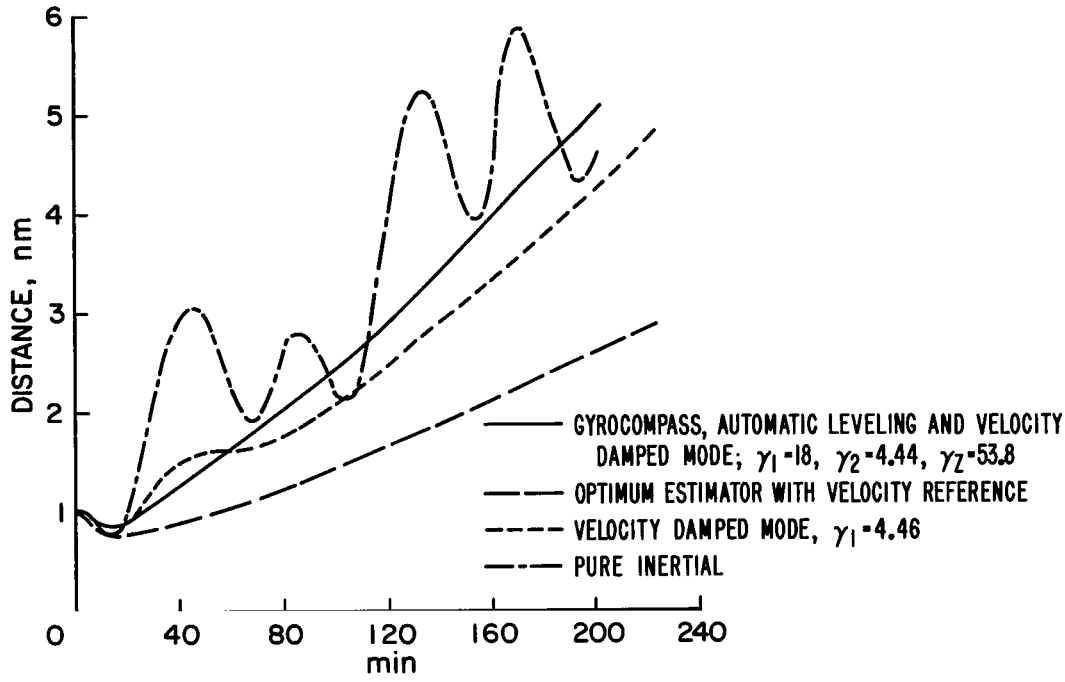

Figure 5.- Propagation of rms longitude error in a well alined inertial navigator (case 2).

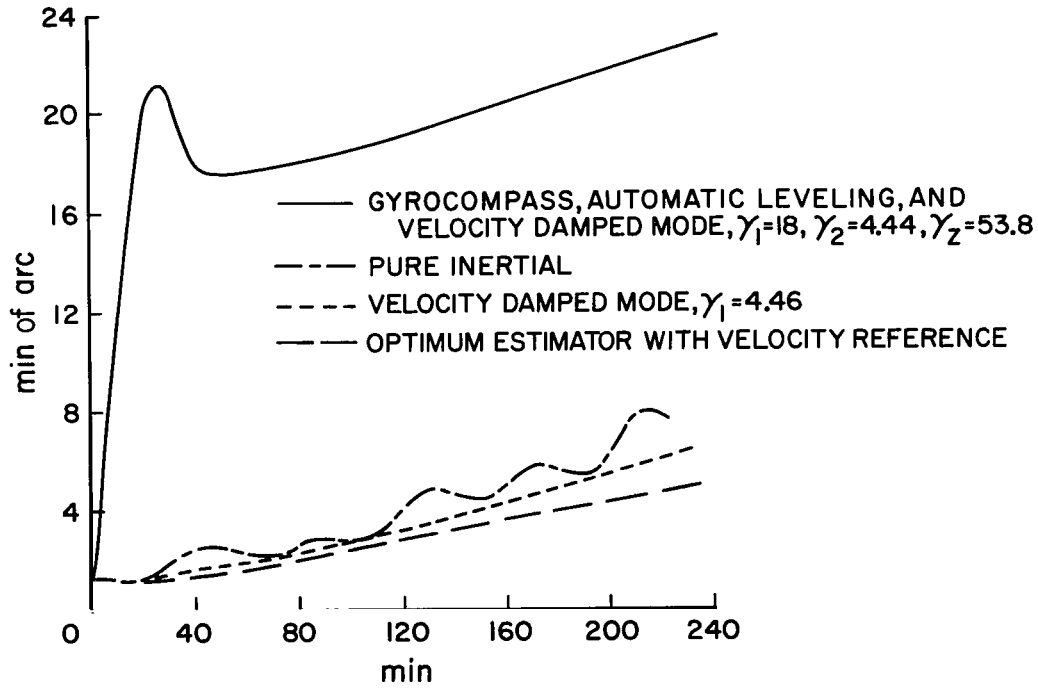

Figure 6.- Propagation of rms azimuth error in a well alined inertial navigator (case 2).

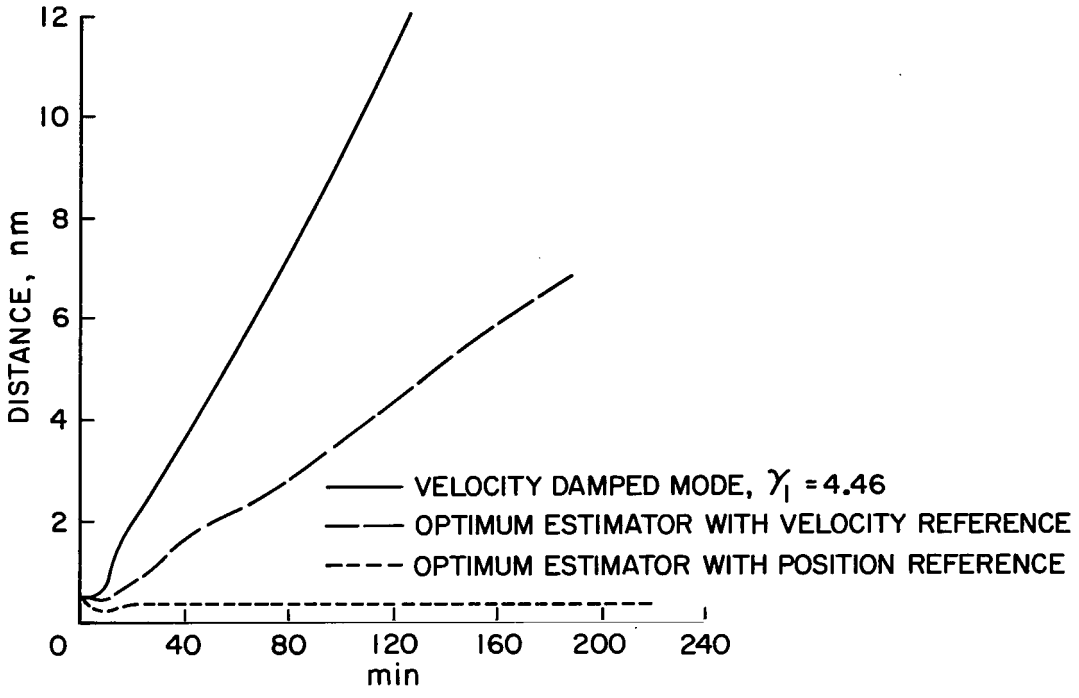

Figure 7.- Propagation of rms latitude error in a fast moving inertial navigator (case 3).

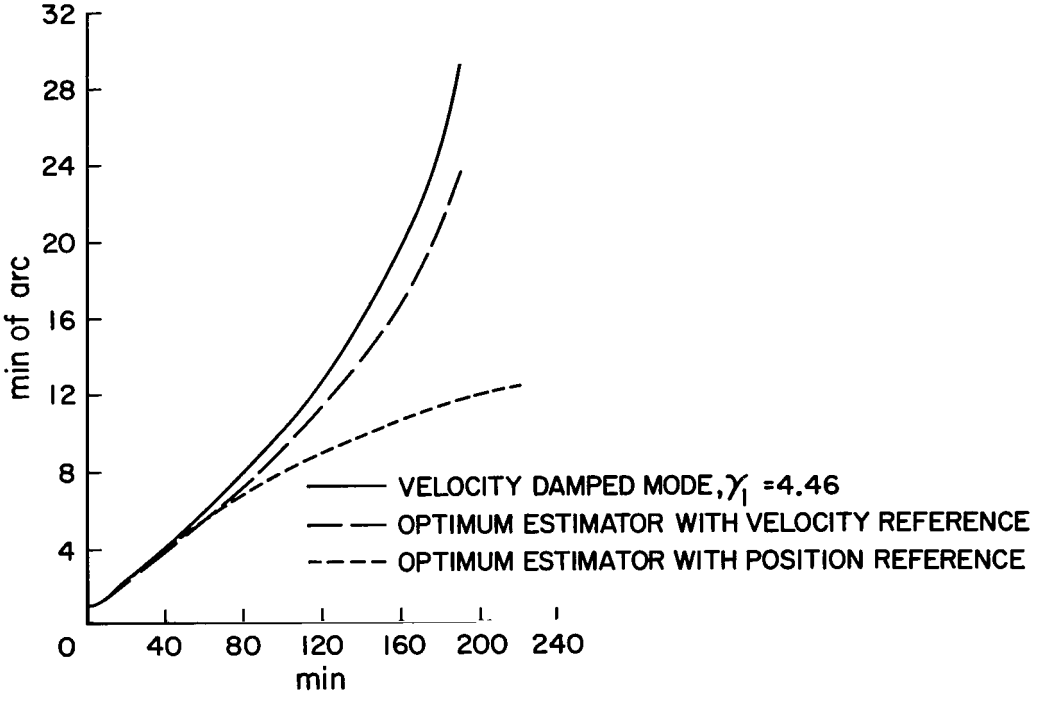

Figure 8.- Propagation of rms azimuth error in a fast moving inertial navigator (case 3).

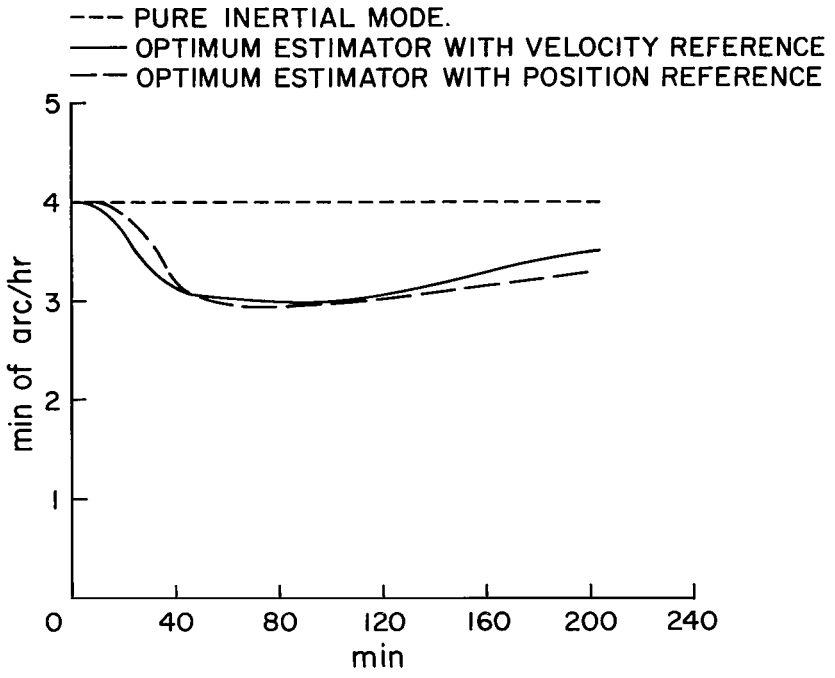

Figure 9.- Constant drift rate about rms polar axis in a fast moving inertial navigator (case 3).